

Stochastic Chiral Polymerization in Open Systems

Marcelo Gleiser and Bradley J. Nelson

Department of Physics and Astronomy, Dartmouth College Hanover, NH 03755, USA

Sara Imari Walker

NASA Astrobiology Institute, USA and

BEYOND: Center for Fundamental Concepts in Science, Arizona State University, Tempe, AZ

We investigate the possibility that prebiotic homochirality can be achieved through stochastic fluctuations of chiral-selective reaction rate parameters. Specifically, we examine an open network of polymerization reactions, where the reaction rates can undergo stochastic fluctuations about their mean values. Varying both the mean value and the rms dispersion of the relevant reaction rates, we show that moderate to high levels of chiral excess can be achieved. Considering the various unknowns related to prebiotic chemical networks in early Earth and the dependence of reaction rates to environmental properties such as temperature and pressure variations, we argue that homochirality could have been achieved via simple stochastic processes.

I. INTRODUCTION

The origin of life on Earth is a central scientific question of our time [1, 2]. A possible way of organizing its many facets is to separate it into three basic aspects, all still unknown: when did it happen; where did it happen; and how did it happen. The “when” question is, to a certain extent, the best understood. We can put a lower limit on the origin of life on Earth at about 3.5 billion years ago (BYA) [3]. Possible evidence of earlier life, dated at 3.8 BYA, remains controversial [4]. Of course, it is also possible that life emerged more than once before this time, although if it did it was probably made extinct quickly due to the unstable conditions of a crustless primeval Earth. At about 3.9 BYA, the Late Heavy Bombardment caused by the displacement of outer planets, constitutes a serious obstacle against any long-term survivability of earlier life forms [5].

The “where” question has many possible answers, ranging from shallow water pools and hot water vents to clay and mineral surfaces [6]. It is also speculated that life may have originated in outer space, possibly Mars [7], and was transplanted to Earth via meteoritic impacts [8]. If not life itself, at least some of its basic organic ingredients may indeed have come from outer space, possibly seeding early life here [9, 10].

The “how” question remains quite open and it may never be answered precisely, as it depends on the details of a prebiotic biochemistry we may never completely know. However, the uniformity in the biochemistry of all living organisms strongly suggests that all life descended from a last-common ancestor (LCA), that lived 3.2-3.8 BYA and had a level of complexity similar to that of a simple modern bacterium [2]. To “explain” the origin of life requires us to explain how abiotic organic compounds combined to generate the first LCA, at present a major challenge.

A key aspect of all terrestrial life is its biomolecular homochirality [11]: the vast majority of amino acids comprising living creatures are levorotatory (L), while the majority of sugars are dextrorotatory (D). Given the link of present and past life to the LCA, we should thus expect that the LCA displayed the same chiral signature as modern life. To explain the origin of life we must also therefore explain the origin of homochirality. Although it is possible that biomolecular homochirality evolved during, or even after, prebiotic chemistry reached a more complex stage as, say, when the first nucleic acids were being formed [12], it is more likely that homochirality is a precondition to life. Accordingly, we will assume here that chiral selectivity played a key role as prebiotic biochemistry began to evolve, setting the conditions for the first living forms to emerge. Within this framework, to understand the “how” question we must first understand the homochiral question: essentially, we must understand how the first homochiral polymers formed under prebiotic conditions.

Over the past decades, several explanations have been offered to account for the homochirality of living organisms [11]. All of them assume that the essential reactions leading to homochirality are highly nonlinear and unstable to growth, so that a small excess of one handedness can be efficiently amplified to full homochirality. There are thus two basic aspects of the homochiral question: first, the cause for the initial excess of one handedness over the other; and second, the amplification mechanism.

Causes for the initial chiral excess can be classified as endogenous or exogenous. By endogenous causes we mean those that are intrinsic to the physics and/or chemistry of the reactor pool. For example, parity symmetry breaking in the weak nuclear interactions has been proposed as a possible source of the initial homochiral excess [13, 14, 15], although the numbers obtained in quantum computations using perturbed Hamiltonians are exceedingly small [16]. Examples of exogenous sources of initial chiral bias include circularly-polarized UV light from active star formation regions [18], and deposits of chiral compounds by meteoritic bombardment [10, 19].

At this point, the debate is still open as to whether any of these possible sources of chiral bias was present at prebiotic times and, if it was, whether it was efficient or necessary. Gleiser, Walker, and Thorarinson have recently argued [20] that even if an initial chiral excess was produced by any of these (or other) mechanisms, environmental disturbances could have erased it, restoring either achiral conditions or switching chirality in the opposite direction: chiral selection might be the result of a series of stochastic reversals prompted by large temperature and/or density fluctuations, or other possible environmental effects. Accordingly, the question of biological homochirality cannot be separated from the details of planetary history. The same conclusion holds for any other planetary platform displaying stereochemistry.

The second basic aspect of the homochiral question focuses on the details of the amplification mechanism. Ever since the seminal work by Frank [21], most of the models attempt to describe how a small chiral bias can be efficiently amplified toward homochirality. Such models rely on a combination of two properties: the reactions must be autocatalytic, thus guaranteeing the nonlinear behavior needed for amplification, and they must display enantiomeric cross-inhibition, that is, enantiomers of opposite chirality can combine, suppressing the growth of heterochiral chains [22, 23, 24]. Within this framework, one must still appeal to a mechanism for generating an initial excess. Traditional approaches along these lines have held that the initial symmetry breaking is endogenous, occurring at the level of small stochastic fluctuations in the concentrations of left- and right-handed monomers, which must then be amplified by the combined effects of autocatalysis and cross-inhibition to yield an appreciable enantiomeric excess [17, 22]. However, fluctuations between the concentrations of left- and right-handed enantiomers may be exceedingly small in a large reactor pool, thereby requiring strong autocatalytic feedback for amplification to occur, if it does at all. Autocatalytic feedback leading to significant chiral selection has only been observed in a few abiotic systems [24], and has not yet been observed in a prebiotically relevant scenario. Consequently, it is prudent to explore other possibilities for the onset of chiral selection in a prebiotic environment.

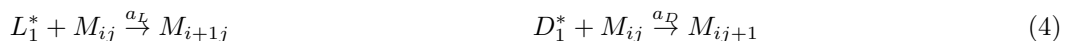
In this work we therefore explore an alternative scenario for the generation of a chiral excess in open polymerization systems, and present a model with chiral-selective reaction rates where chiral selectivity is randomly determined by stochastic fluctuations about the mean values of the reaction rates. In this framework, a large statistical sampling of the systems under study would on average be racemic; however, stochastic variations in reaction rates lead to significant chiral excess for some members of the sampled ensembles. Within a prebiotic scenario on early Earth, we might imagine that such fluctuations in the reaction rates were prompted by environmental disturbances. Thus, we will explore the possibility that terrestrial biomolecular homochirality might have arisen stochastically, without the need for any specific chiral biasing or amplification mechanism. For illustrative values of the relevant reaction rates, we will place lower bounds on the amplitude of fluctuating reaction rates needed for substantial chiral bias.

II. CHIRAL POLYMERIZATION MODEL

Consider a polymerization reaction network where activated levorotatory and dextrorotatory monomers (L_1^* and D_1^* , respectively) can chain up to generate longer homochiral or heterochiral molecules. The model reactions include deactivation of activated monomers,



and the polymerization reactions,



where $h_{L(D)}$ is the deactivation rate for $L(D)$ -monomers and $a_{L(D)}$ is the polymerization rate for adding activated $L(D)$ -monomers to a growing chain. Here L_i and D_j denote homochiral polymers of length i and j respectively, and M_{ij} denotes polymers of mixed chirality consisting of i L -monomers and j D -monomers.

In general, the temperature dependence of reaction rates is determined by the Arrhenius factor, $k \sim \exp[-E_a/RT]$, where E_a is the activation energy related to departures from equilibrium populations of molecules. Thus, if $k_{L(R)}$ represents some general reaction rate concerning $L(D)$ enantiomers, and if Δ is the difference in their activation energy biasing L -enantiomers, then $k_L/k_D = \exp[\Delta/RT]$. A local fluctuation in temperature in a region richer in one of the two enantiomers can drive reactions faster for one chirality. Given that details of prebiotic chemistry remain elusive, we are considering that, in principle, reaction rates may be chiral-selective. However, instead of assigning *ad hoc* values for the rates of opposite chirality, we will conduct a stochastic analysis whereby, for different numerical experiments, the values for L and D reactions rates will be allowed to randomly fluctuate about a given mean. In

other words, each time we solve the coupled nonlinear ordinary differential equations describing the reactions, we will pick random, Gaussian-distributed values for the reactions rates $h_{L(D)}$ and $a_{L(D)}$. This will allow us to investigate the range in the reaction rates that generate a substantial departure from racemic results. As we will see, modest values for the fluctuation range will suffice to generate substantial chiral bias. These fluctuations may be triggered by conformational differences between levorotatory and dextrorotatory reactivity, from purely statistical fluctuations [25], or due to environmental influences on the reactions that may bias one handedness over the other. The latter can be representing seeding from meteoritic materials, chiral-selective temperature sensitivity, or chiral photolysis.

In practice, we will consider pairs of randomly-distributed reaction rates (h_L, h_D) and (a_L, a_D) taken from a Gaussian distribution with a racemic mean

$$\begin{aligned}\langle h_L \rangle &= \langle h_D \rangle = \bar{h} \\ \langle a_L \rangle &= \langle a_D \rangle = \bar{a},\end{aligned}\tag{5}$$

and a two-point correlation

$$\begin{aligned}\langle h_{L(D)} h_{L'(D')} \rangle &= h_0^2 \delta_{LL'(DD')} \\ \langle a_{L(D)} a_{L'(D')} \rangle &= a_0^2 \delta_{LL'(DD')},\end{aligned}\tag{6}$$

where h_0 and a_0 are the rms values, and $\delta_{xx'}$ is the Kronecker delta. The angled brackets mean an average over N experiments (an ensemble average), with N large. For example, the normalized probability $P(h_L)$ that the L -hydrolysis rate will obtain a value h_L is

$$P(h_L) = \frac{1}{\sqrt{2\pi h_0^2}} \exp[-(h_L - \bar{h})^2 / 2h_0^2].\tag{7}$$

In the open systems studied here we also include the additional rates S describing the permeation of activated L_1^* and D_1^* monomers into the system, and d describing the loss of all molecular species from the system. For closed systems $S = d = 0$.

For the above system, the rate equations for the various concentrations are written as (from now on, quantities in capitals denote the concentrations of the different reactants):

$$\frac{dL_1^*}{dt} = S - h_L L_1^* - a_L L_1^* \left(\sum_{i=1}^{\infty} L_i + \sum_{j=1}^{\infty} D_j + \sum_{i=1}^{\infty} \sum_{j=1}^{\infty} M_{ij} \right) - dL_1^* \tag{8}$$

$$\frac{dD_1^*}{dt} = S - h_D D_1^* - a_D D_1^* \left(\sum_{i=1}^{\infty} L_i + \sum_{j=1}^{\infty} D_j + \sum_{i=1}^{\infty} \sum_{j=1}^{\infty} M_{ij} \right) - dD_1^* \tag{9}$$

$$\frac{dL_1}{dt} = h_L L_1^* - a_L L_1 L_1^* - a_D L_1 D_1^* - dL_1 \tag{10}$$

$$\frac{dD_1}{dt} = h_D D_1^* - a_L D_1 L_1^* - a_D D_1 D_1^* - dD_1 \tag{11}$$

$$\frac{dL_i}{dt} = a_L L_1^* L_{i-1} - a_L L_i L_1^* - a_D L_i D_1^* - dL_i \quad (i \geq 2) \tag{12}$$

$$\frac{dD_j}{dt} = a_D D_1^* D_{j-1} - a_L D_j L_1^* - a_D D_j D_1^* - dD_j \quad (j \geq 2) \tag{13}$$

$$\frac{dM_{ij}}{dt} = a_L L_1^* M_{i-1j} + a_D D_1^* M_{ij-1} - a_L M_{ij} L_1^* - a_D M_{ij} D_1^* - dM_{ij} \quad (i \geq 1, j \geq 1) \tag{14}$$

We can simplify the reactions above by defining

$$\mathcal{L} = \sum_{i=2}^{\infty} L_i, \quad \mathcal{D} = \sum_{j=2}^{\infty} D_j, \quad \mathcal{M} = \sum_{i=1}^{\infty} \sum_{j=1}^{\infty} M_{ij}, \tag{15}$$

and summing the reaction equations over i and j . Then the reaction-network, in the limit of infinite-length polymers,

reduces to:

$$\frac{dL_1^*}{dt} = S - h_L L_1^* - a_L L_1^* (L_1 + \mathcal{L} + D_1 + \mathcal{D} + \mathcal{M}) - dL_1^*; \quad (16)$$

$$\frac{dD_1^*}{dt} = S - h_D D_1^* - a_D D_1^* (L_1 + \mathcal{L} + D_1 + \mathcal{D} + \mathcal{M}) - dD_1^*; \quad (17)$$

$$\frac{dL_1}{dt} = h_L L_1^* - a_L L_1 L_1^* - a_D L_1 D_1^* - dL_1; \quad (18)$$

$$\frac{dD_1}{dt} = h_D D_1^* - a_L D_1 L_1^* - a_D D_1 D_1^* - dD_1; \quad (19)$$

$$\frac{d\mathcal{L}}{dt} = a_L L_1^* L_1 - (a_D D_1^* + d)\mathcal{L}; \quad (20)$$

$$\frac{d\mathcal{D}}{dt} = a_D D_1^* D_1 - (a_L L_1^* + d)\mathcal{D}; \quad (21)$$

$$\frac{d\mathcal{M}}{dt} = a_L L_1^* (D_1 + \mathcal{D}) + a_D D_1^* (L_1 + \mathcal{L}) - d\mathcal{M}. \quad (22)$$

The quantity of interest is the enantiomeric excess $[ee(t)]$, that is, the net chirality, which we define as

$$ee(t) = \frac{[L_1^*(t) + L_1(t) + \mathcal{L}(t)] - [D_1^*(t) + D_1(t) + \mathcal{D}(t)]}{[L_1^*(t) + L_1(t) + \mathcal{L}(t)] + [D_1^*(t) + D_1(t) + \mathcal{D}(t)]}. \quad (23)$$

Note that our definition of the enantiomeric excess implicitly assumes that we are only interested in pure homochiral polymers. Given initial values for the concentrations, the equations describing their evolution can be solved and the net chirality computed as a function of time. We will choose the simplest possible initial conditions, setting all initial concentrations to zero, with the exception of $L_1^*(0)$ and $D_1^*(0)$, which we will set equal to each other so that the system starts with no chiral bias and no long polymer chains. We will also pick a constant value for the source for activated monomers, $S(t) = S$. With this choice, we will be able to investigate under which conditions, that is, values for the reaction rates, the system engenders a net chirality as it evolves to a steady-state wherein all concentrations achieve a dynamic equilibrium so that their time derivatives vanish. Before we show solutions to the system of equations, we note that we can eliminate the death rate d from the equations, dividing them on both sides by it. Since d has dimensions of inverse time, this is equivalent to introducing the dimensionless time variable $\tau = td$ so that we can write the equations as,

$$\frac{dL_1^*}{d\tau} = \sigma - \beta_L L_1^* - \alpha_L L_1^* (L_1 + \mathcal{L} + D_1 + \mathcal{D} + \mathcal{M}) - L_1^*; \quad (24)$$

$$\frac{dD_1^*}{d\tau} = \sigma - \beta_D D_1^* - \alpha_D D_1^* (L_1 + \mathcal{L} + D_1 + \mathcal{D} + \mathcal{M}) - D_1^*; \quad (25)$$

$$\frac{dL_1}{d\tau} = \beta_L L_1^* - \alpha_L L_1 L_1^* - \alpha_D L_1 D_1^* - L_1; \quad (26)$$

$$\frac{dD_1}{d\tau} = \beta_D D_1^* - \alpha_L D_1 L_1^* - \alpha_D D_1 D_1^* - D_1; \quad (27)$$

$$\frac{d\mathcal{L}}{d\tau} = \alpha_L L_1^* L_1 - (\alpha_D D_1^* + 1)\mathcal{L}; \quad (28)$$

$$\frac{d\mathcal{D}}{d\tau} = \alpha_D D_1^* D_1 - (\alpha_L L_1^* + 1)\mathcal{D}; \quad (29)$$

$$\frac{d\mathcal{M}}{d\tau} = \alpha_L L_1^* (D_1 + \mathcal{D}) + \alpha_D D_1^* (L_1 + \mathcal{L}) - \mathcal{M}, \quad (30)$$

where we have introduced $\sigma \equiv S/d$, $\alpha_{L(D)} \equiv a_{L(D)}/d$, and $\beta_{L(D)} \equiv h_{L(D)}/d$. With this parametrization $\alpha_0 = a_0/d$, $\beta_0 = h_0/d$, and $\bar{\alpha} = \bar{a}/d$ and $\bar{\beta} = \bar{h}/d$ characterize the random distributions of reaction rates outlined in eqs. 5 and 6. Thus, all reaction rates and dynamical time-scales are expressed in terms of the disappearance rate d . In particular, σ gives the ratio per unit volume of entrance versus exiting of reacting materials to and from the reactor pool.

III. RESULTS

In Figure 1 we show the behavior of the time evolution of enantiomeric excess for several illustrative examples with $\sigma = 200$ and different choices for the reaction rates α_L , α_D , β_L and β_D . On the left, we show results with

$\beta_L = \beta_D = 100$ fixed, and varying ratios of α_L/α_D . Shown are the results for $\alpha_L = 5.0$, $\alpha_D = 10.0$ ($\alpha_L/\alpha_D = \frac{1}{2}$) in blue, $\alpha_L = 5.0$, $\alpha_D = 15.0$ ($\alpha_L/\alpha_D = \frac{1}{3}$) in black, and $\alpha_L = 5.0$, $\alpha_D = 20.0$ ($\alpha_L/\alpha_D = \frac{1}{4}$) in red. The system quickly reaches a steady state with net chiral excess $ee_{ss} \simeq 0.24$, $ee_{ss} \simeq 0.38$, and $ee_{ss} \simeq 0.48$, respectively (corresponding to 24%, 38%, and 48% enantiomeric excess). On the right, we show results holding $\alpha_L = \alpha_D = 10.0$ fixed, and varying the ratio of β_L/β_D . Shown are the results for $\beta_L = 75$, $\beta_D = 25$ ($\beta_L/\beta_D = 3$) in blue, $\beta_L = 100$, $\beta_D = 25$ ($\beta_L/\beta_D = 4$) in black, and $\beta_L = 125$, $\beta_D = 25$ ($\beta_L/\beta_D = 5$) in red. In this case the net chiral excess at steady-state is $ee_{ss} \simeq 0.38$, $ee_{ss} \simeq 0.47$, and $ee_{ss} \simeq 0.58$, respectively (corresponding to 38%, 47%, and 58% enantiomeric excess). These test runs show that for differing left and right reaction rates a substantial amount of chiral excess may be reached at steady-state.

In general, we note the reactions favor an L -excess for ratios $\alpha_L/\alpha_D < 1$ and/or $\beta_L/\beta_D > 1$ as demonstrated by the results shown in Figure 1. At first glance this may seem counterintuitive, particularly the relationship between α_L/α_D and the net enantiomeric excess of homochiral polymers. Intuitively one would expect that increasing α_D (the polymerization rate of activated D -monomers) while holding α_L (the polymerization rate of activated L -monomers) fixed would result in a net excess favoring D , and not L as observed. However, on closer inspection one must note that α_D describes the rate of attachment of activated D -monomers to growing D - or L - chains, leading to higher yields of D -enriched mixed polymers and a correspondingly lower yield of pure D -polymers. Likewise, increasing the deactivation rate of L -monomers (*i.e.* β_L) and thereby increasing the ratio β_L/β_D leads to fewer L -activated monomers for polymerization which decreases the yield of pure homochiral L - polymers, but also decreases the loss of L -monomers to polymers of mixed chirality, resulting in a net increase in the enantiomeric excess favoring L . Clearly, with the same values of L and D reaction rates, $ee = 0$ for all t . We must thus examine how the results behave for statistical samplings of α_L , α_D , β_L , and β_D .

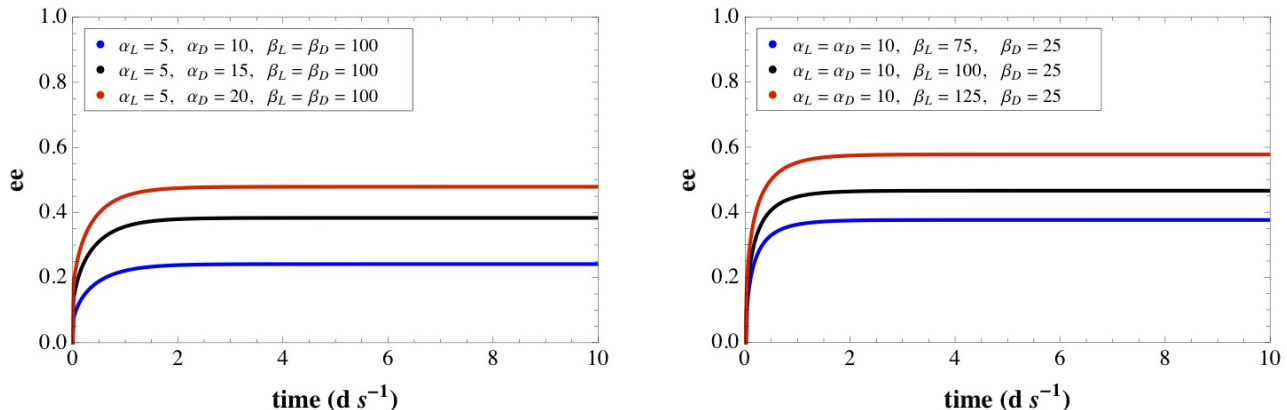


FIG. 1: Time evolution of enantiomeric excess for illustrative examples of reaction rates with $\sigma = 200$. **Left:** $\beta_L = \beta_D = 100$, with varying ratios of α_L/α_D . Shown are $\alpha_L = 5.0$, $\alpha_D = 10.0$ ($\alpha_L/\alpha_D = \frac{1}{2}$) in blue, $\alpha_L = 5.0$, $\alpha_D = 15.0$ ($\alpha_L/\alpha_D = \frac{1}{3}$) in black, and $\alpha_L = 5.0$, $\alpha_D = 20.0$ ($\alpha_L/\alpha_D = \frac{1}{4}$) in red. **Right:** $\alpha_L = \alpha_D = 10.0$, with varying ratios of β_L/β_D . Shown are $\beta_L = 75$, $\beta_D = 25$ ($\beta_L/\beta_D = 3$) in blue, $\beta_L = 100$, $\beta_D = 25$ ($\beta_L/\beta_D = 4$) in black, and $\beta_L = 125$, $\beta_D = 25$ ($\beta_L/\beta_D = 5$) in red

We have performed a detailed statistical study of the reaction equations with fluctuating values for the L - and D -reaction rates α_L , α_D , β_L and β_D as described in eqs. 5 and 6 scaled by d . This involves solving the coupled system of ordinary differential equations above (eqns. 24–30) N times, each with values for the four reaction rates given by $\alpha_L = \bar{\alpha} + \delta_L$, $\alpha_D = \bar{\alpha} + \delta_D$, $\beta_L = \bar{\beta} + \xi_L$, and $\beta_D = \bar{\beta} + \xi_D$, where the bars denote the mean values (cf. eq. 5) and $\delta_{L(D)}$ and $\xi_{L(D)}$ are Gaussian-distributed random numbers (cf. eq. 6), within a fixed rms width set by α_0 and β_0 .

Our results indicate that the net chirality is overall more sensitive to the amplitude of the fluctuations than to the mean values of the reaction rates. In Figures 2 and 3 we show the results for three sets of data with fluctuations in $\beta_{L(D)}$ varying between 10% and 30% (*i.e.* $0.1 \leq \beta_0 \leq 0.3$) and fluctuations in $\alpha_{L(D)}$ fixed at 20% (*i.e.* $\alpha_0 = 0.2$). Each data point represents an ensemble average over a random sample of $N = 5000$ individual experiments. Shown are results for $\bar{\alpha} = 10$, $\bar{\beta} = 100$ in blue, $\bar{\alpha} = 15$, $\bar{\beta} = 90$ in red, and $\bar{\alpha} = 20$, $\bar{\beta} = 120$ in black. Figure 2 demonstrates that the ensemble-averaged enantiomeric excess is racemic, with an equal number of systems favoring excesses in D as in L , as should be expected. Closer inspection of the details of the distribution demonstrate that some chemistries within the statistical sampling have moderate to large enantiomeric excesses. In Figure 3a, the mean value of the net chirality is shown (*i.e.* the mean *magnitude* of the enantiomeric excess). Although the distribution of enantiomeric excess is centered on zero as shown in Figure 2, Figure 3a demonstrates that the average net chiral asymmetry obtains moderate values, with the $\langle |ee| \rangle$ varying from $\sim 10\%$ for $\beta_0 = 0.1$ to $\sim 16\%$ for $\beta_0 = 0.3$, with the $\langle |ee| \rangle$ increasing nearly linearly with the size of the fluctuations. We stress that individual members of the ensemble may have much

larger net chiralities than these mean values. The variances of the data set are shown in Figure 3b, and range between ~ 0.015 and ~ 0.045 for $\beta_0 = 0.1$ and $\beta_0 = 0.3$, respectively. As with the mean value of the net chirality, the variance increases with the amplitude of fluctuations, leading to a wider spread in the values of the enantiomeric excess with increasing β_0 . For large fluctuations, say $\beta_0 = 0.3$, the variance is ~ 0.04 , corresponding to a standard deviation of 0.2, indicating that 68% of systems have an $|ee| < 0.2$, and 27% have an enantiomeric excesses in the range $0.2 \leq |ee| \leq 0.4$ (assuming a normal distribution for the data, see Figure 4). A small fraction of 0.2% of systems possess a sizable $|ee|$ in excess of 0.6.

In Figure 4, we further explore the spread in the distribution of the enantiomeric excess in experimental systems for an example ensemble with $\bar{\alpha} = 20$, $\bar{\beta} = 120$ and $\alpha_0 = \beta_0 = 0.25$. Outliers in the distribution have very high enantiomeric excesses up to as much as 80 – 90%. However, most systems fall within a range of enantiomeric excesses with $|ee| < 0.25$, where the mean of the distribution lies. In Figure 5, we show a surface plot of the mean values of the net chiral asymmetry for $\beta_{L(D)}$ varying between 10% and 30% (*i.e.* $0.1 \leq \beta_0 \leq 0.3$) and fluctuations in $\alpha_{L(D)}$ varying over the same range. The highest values for the net enantiomeric excess are observed for large fluctuations in $\alpha_{L(D)}$ and $\beta_{L(D)}$, where mean values for the net enantiomeric excess reach as high as $|ee| \sim 0.2$ for the systems under study. These results demonstrate a general trend of increased average $\langle |ee| \rangle$ with increased fluctuation sizes, as well as an increase in the spread of the distribution, indicating that larger fluctuations lead to a larger fraction of outliers with significant enantiomeric excess.

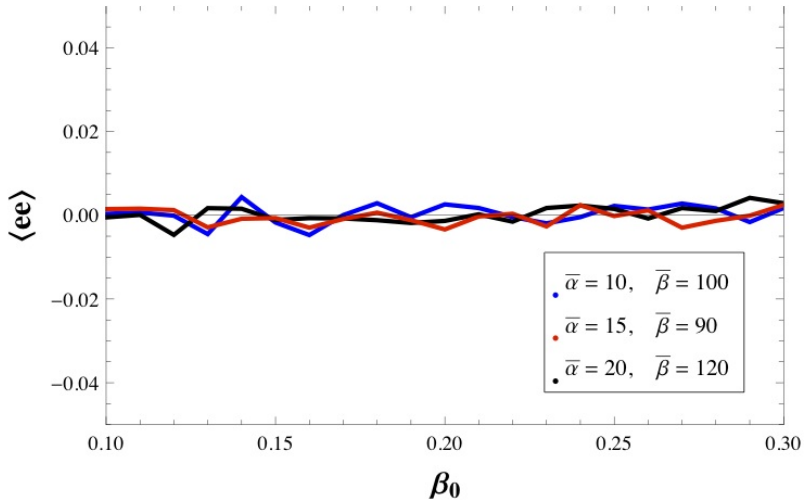


FIG. 2: Ensemble averaged enantiomeric excess, $\langle ee \rangle$, for sample sizes $N = 5000$ and fluctuations in $\alpha_{L(D)}$ fixed at 20% ($\alpha_0 = 0.2$), with fluctuations in $\beta_{L(D)}$ varying between 10% and 30% ($0.1 \leq \beta_0 \leq 0.3$) and fixed $\sigma = 200$. Shown are $\bar{\alpha} = 10$, $\bar{\beta} = 100$ in blue, $\bar{\alpha} = 15$, $\bar{\beta} = 90$ in red, and $\bar{\alpha} = 20$, $\bar{\beta} = 120$ in black.

IV. SUMMARY AND OUTLOOK

Due to the symmetry between the chemistries of L - and D - monomers, including the biologically relevant examples of amino acids and nucleotides, it is expected that nearly all chemical interactions between the two enantiomeric forms and their environment are symmetric with respect to both chiralities. However, specific local environmental influences, such as mineral surfaces, chiral-selective temperature sensitivity, photolysis, or the presence of asymmetric catalysts, can bias reactions to favor one chirality over the other. All of these examples are inherently globally symmetric, such that on average a statistical sampling of chemistries will be racemic (*i.e.* some will favor L and others D). Asymmetry therefore arises depending on the particular context. For example, surfaces can lead to chiral-selectivity due to differential activity of the two enantiomers when adhered to minerals or clays [26, 27]. This can lead specific local chemistries to have fluctuations in reaction rates that differ significantly from the standard reactivities in free solution. We have explored such scenarios here, within the context of the as yet unknown prebiotic chemistry which may have given rise to the first life-forms. As we have shown, different environmental contexts will lead to varying deviations from the mean reactivity of L - and D - enantiomers, leading to localized symmetry breaking which is directly dependent on the environmental context. Larger fluctuations will result in some chemistries having substantial chiral asymmetries. Based on the results presented here, we expect that fluctuations of at least 10% in reactivities of L - and D - monomers are required to lead to significant chiral symmetry breaking (*i.e.* $|ee| > 10\%$).

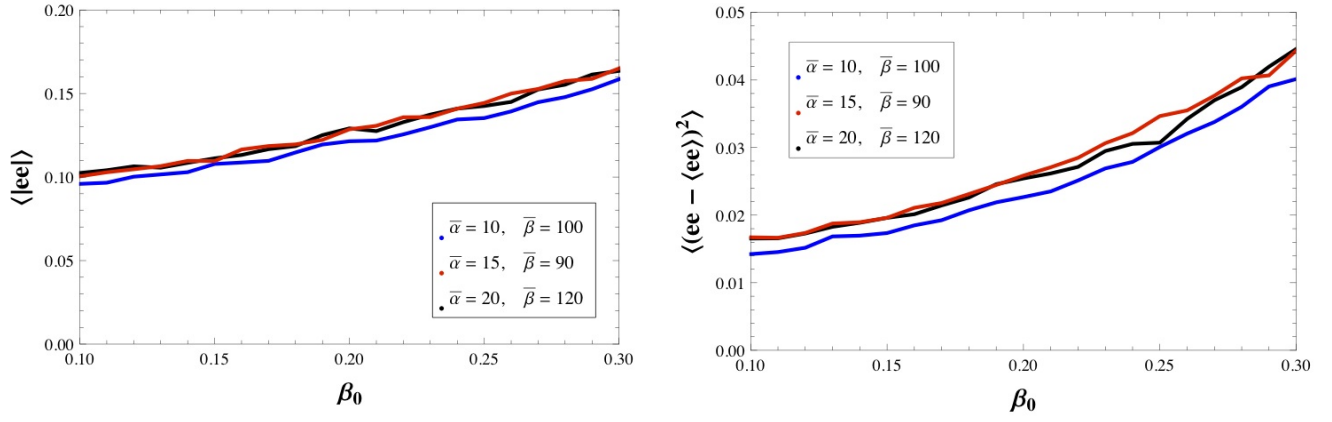


FIG. 3: Ensemble averaged mean of the net enantiomeric excess, $\langle |ee| \rangle$, and variance for the ensemble data shown in Figure 2 with $N = 5000$, with fluctuations in $\alpha_{L(D)}$ fixed at 20% ($\alpha_0 = 0.2$), and fluctuations in $\beta_{L(D)}$ varying between 10% and 30% ($0.1 \leq \beta_0 \leq 0.3$) and fixed $\sigma = 200$. Shown are $\bar{\alpha} = 10$, $\bar{\beta} = 100$ in blue, $\bar{\alpha} = 15$, $\bar{\beta} = 90$ in red, and $\bar{\alpha} = 20$, $\bar{\beta} = 120$ in black. **Left:** Mean values of the net enantiomeric excess, $\langle |ee| \rangle$. **Right:** Variance in the enantiomeric excess $\langle (ee - \langle ee \rangle)^2 \rangle$.

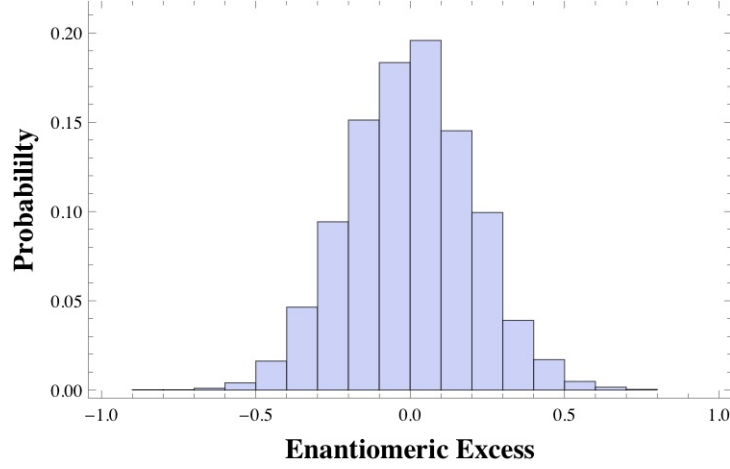


FIG. 4: Distribution of ensemble ee values for $N = 5000$ with $\bar{\alpha} = 20$, $\bar{\beta} = 120$, $\alpha_0 = \beta_0 = 0.25$, and $\sigma = 200$.

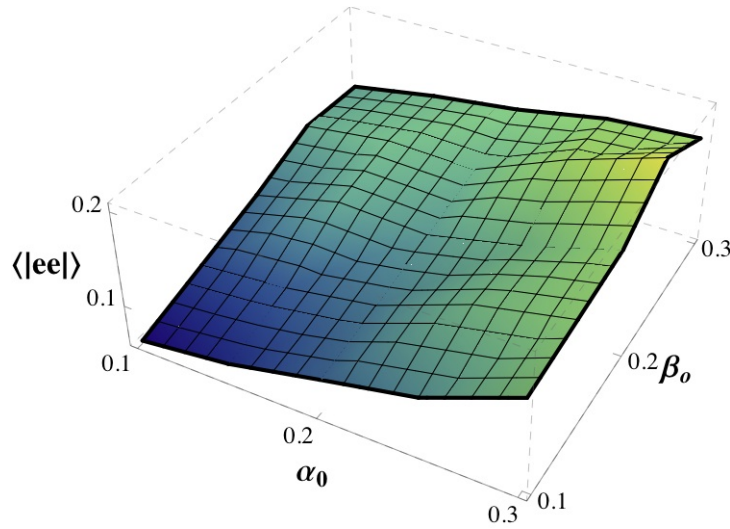


FIG. 5: Ensemble averaged net enantiomeric excess, $\langle |ee| \rangle$, for $N = 100$ with fluctuations in $\alpha_{L(D)}$ and $\beta_{L(D)}$ between 10% and 30% (α_0, β_0 between 0.1 and 0.3) with $\bar{\alpha} = 20$, $\bar{\beta} = 200$ and $\sigma = 200$.

Additionally, fluctuations in chiral-selective reaction rates, may provide an alternative mechanism to the initiation of chiral asymmetry prior to amplification via autocatalysis with enantiomeric cross-inhibition in a Frank-type mechanism. Traditional approaches assume that fluctuations in the relative numbers of *L*- and *D*- monomers are enough to break the initial symmetry between the two enantiomers, which may then be amplified. However, fluctuations in chemical systems typically scale as $1/\sqrt{N}$ [28], where N is the number of molecules in the system, and will therefore be exceedingly small for most chemical systems. Deviations from perfect racemates will therefore be extremely small and require significant enzymatic enhancement by efficient catalysts to be amplified (*e.g.* see [17]). Here we present an alternative and more robust mechanism for symmetry breaking, whereby the initial symmetry breaking occurs at a macroscopic rather than microscopic level, being a manifestation of fluctuations in reactivities, rather than in molecular numbers. Such scenarios obviate the need for special asymmetric initial conditions, allowing asymmetry to emerge as the reactions unfold, due to asymmetries present in the local chemistry.

Finally, we note that our results suggest that the origin of homochirality on the prebiotic Earth was a statistical process, potentially hosting many abiogenic events, few of which were highly asymmetric. Likely, only those chemistries which were highly asymmetric were capable of giving rise to life [11], and only one of these trials ultimately led to the emergence of the LCA. This has different observational consequences for experimental systems as well as searches for biosignatures on other worlds than the exogenous or endogenous sources of chiral excess described above. Parity-violation would result in a universal bias toward a particular chiral asymmetry, while UV-irradiation might lead to chiral biases on the scale of planetary systems. Here chiral selectivity is a local statistical phenomena, and we should expect a large sampling of extraterrestrial stereochemistries to be racemic on average.

Acknowledgements

MG is supported in part by a National Science Foundation grant PHY-1068027. BJN is a Presidential Scholar at Dartmouth College. SIW gratefully acknowledges support from the NASA Astrobiology Institute through the NASA Postdoctoral Fellowship Program.

-
- [1] Sullivan, W. T. III and Baross, J, Eds., *Planets and Life: The Emerging Science of Astrobiology*, Cambridge University Press: Cambridge, 2007.
 - [2] Orgel, L. E., The Origin of Life: a review of facts and speculation. In *The Nature of Life*; Bedau, M. A., and Cleland, C. E., Eds.; Cambridge University Press: Cambridge, 2010; pp. 121-128.
 - [3] Mojzsis, S. J., Arrhenius, G., McKeegan, K. D., Harrison, T. M., Nutman, A. P., and Friend, C. R. *Nature***1996**,*384*, 55-59.
 - [4] van Zuilen, M. A., Lepland, A., and Arrhenius, G., *Nature* **420** (2002) 202.
 - [5] Gomes, R., Levinson, H. F., Tsiganis, K., and Morbidelli, A., Origin of the cataclysmic Late Heavy Bombardment period of the terrestrial planets. *Nature***2005**,*435*, 466-XXX.
 - [6] Corliss, J. B., Baross, J. A., and Hoffman, S. E., *Oceanologica Acta* **4** (1981) 59.
 - [7] McKay, C. *Cold Spring Harb. Perspect. Biol.* **2** (2010) a003509.
 - [8] Davies, P.C.W., The FIFTH MIRACLE: The Search for the Origin and Meaning of Life. *Simon & Schuster* (2000).
 - [9] Chyba, C. and Sagan, C., *Nature* **355** (1992) 125.
 - [10] Cronin, J. R., and Pizzarello, S., *Science* **275** (1997) 951.
 - [11] Bonner, W. A., The Quest for Chirality, in *Physical Origin of Homochirality in Life*, ed. D. Cline (AIP Conference Proceedings 379, AIP Press, New York, 1995); Fitz, D., Reiner, H., Plakensteiner K., and Rode, B., *Curr. Chem. Biol.* **1** (2007) 41.
 - [12] Gilbert, W., *Nature* **319** (1986) 618.
 - [13] Yamagata, Y., *J. Theoret. Biol.* **11** (1966) 495-498.
 - [14] Salam, A., *J. Mol. Evol.* **33** (1991) 105.
 - [15] Kondepudi, D. K., and Nelson, G. W., *Nature*, **314** (1985) 438-441.
 - [16] Bakasov, A., Ha, T. K., and Quack, M., *J. Chem. Phys.* **109** (1998) 7263.
 - [17] Gleiser M., and Walker, S. I., *Orig. Life Evol. Biosph.* **38** (2008) 293.
 - [18] Bailey, J., *Orig. Life Evol. Biosph.* **31** (2001) 167.
 - [19] Glavin, D.P. and Dworking, J.P. *PNAS* **106** (2009) 5487.
 - [20] Gleiser M., Thorarinson J., and Walker, S. I., *Orig. Life Evol. Biosph.* **38** (2008) 499.
 - [21] Frank, F., *Biochim. Biophys. Acta* **11** (1953) 459.
 - [22] Sandars, P. G. H., *Orig. Life Evol. Biosph.* **33** (2003) 575.
 - [23] Wattis, J. A., and Coveney, P. V., *Orig. Life Evol. Biosph.* **35** (2005) 243.
 - [24] Saito Y. and Hyuga, H., *J. Phys. Soc. Japan* **74** 535.
 - [25] Dunitz, J. D., *PNAS* **93** (1996) 14260.

- [26] Joshi, P.C., Pitsch, S. and Ferris, J. *Orig. Life Evol. Biosph.* **37** (2007) 3.
- [27] Hazen, R. and Sholl, D. *Nature Materials* **2** (2003) 367.
- [28] Landau, L.D. and Lifshitz, E. M. *Statistical Physics*; Butterworth-Heinemann: Oxford, 1980.